Mol Neurobiol (2016) 53:4247–4260
DOI 10.1007/s12035-015-9354-4

# Extremely Low Frequency Magnetic Field (ELF-MF) Exposure Sensitizes SH-SY5Y Cells to the Pro-Parkinson's Disease Toxin $MPP^+$

**Barbara Benassi[1] · Giuseppe Filomeni[2,3] · Costanza Montagna[2,3] · Caterina Merla[1] · Vanni Lopresto[1] · Rosanna Pinto[1] · Carmela Marino[1] · Claudia Consales[1]**

Received: 7 January 2015 / Accepted: 7 July 2015 / Published online: 30 July 2015


**Abstract** Parkinson's disease (PD) is a neurodegenerative disorder characterized by dopaminergic neuron loss, with an etiopathogenesis involving both genetic and environmental factors. The occupational/residential exposure to the electromagnetic fields has been recently associated with an increased risk of neurodegenerative diseases; it has been thus proposed that the extremely low frequency magnetic field (ELF-MF) may contribute to neurodegenerative etiopathogenesis, as its interaction with biological systems directly impairs redox homeostasis in specific areas of the brain. The molecular mechanisms elicited by ELF-MF, and their potential involvement in PD onset, still remain unclear. To this end, we set up a generator of ELF-MF able to stably and homogeneously reproduce environmental prolonged exposure to ELF-MF (50 Hz, 1 mT). Results obtained indicate that ELF-MF exposure alters cell response of SH-SY5Y cells to $MPP^+$. We demonstrate that ELF-MF does not affect per se survival, shape, and morphology of both proliferating and differentiated SH-SY5Y cells but significantly impairs redox homeostasis and thiol content, triggering an increase in protein carbonylation. As a result, toxicity of $MPP^+$, even at low doses, is highly enhanced in ELF-MF-exposed cells due to a significant increase in ROS levels, potentiation of oxidative damage, and induction of a caspase-dependent apoptosis. Pre-incubation with the thiol antioxidants *N*-acetyl-L-cysteine and GSH ethyl-ester significantly reduces the extent of oxidative damage and protects cells from death induced by the combined treatment ELF-MF/$MPP^+$. Taken overall, our results demonstrate the redox-based molecular interaction between ELF-MF and PD neurotoxins in vitro, and open a new scenario for defining the synergy of environmental factors in PD onset.

**Keywords** Parkinson's disease (PD) · Extremely low frequency magnetic field (ELF-MF) · 1-methyl-4-phenylpyridinium ($MPP^+$) · Oxidative stress · Apoptosis · SH-SY5Y

**Abbreviations**

| | |
|---|---|
| AD | Alzheimer's disease |
| ALS | Amyotrophic lateral sclerosis |
| B field | Induction magnetic field |
| BSO | Buthionine-S,R-sulfoximine |
| CMFDA | 5-chloromethylfluorescein diacetate |
| DAergic | Dopaminergic |
| DHE | Dihydroethidium |
| E field | Electric field |
| ELF-MF | Extremely low frequency magnetic fields |
| GSH | Reduced glutathione |
| GSHest | Reduced glutathione ethyl ester |
| $H_2$-DCFDA | 2′,7′-Dichlorofluorescin diacetate |
| LBs | Lewy bodies |
| MFI | Mean fluorescence intensity |
| $MPP^+$ | 1-methyl-4-phenylpyridinium |
| MPTP | Methyl-4-phenyl-1,2,3,6-tetra-hydropyridine |
| NAC | *N*-Acetyl-L-cysteine |

**Electronic supplementary material** The online version of this article (doi:10.1007/s12035-015-9354-4) contains supplementary material, which is available to authorized users.

✉ Barbara Benassi
barbara.benassi@enea.it

✉ Claudia Consales
claudia.consales@enea.it

[1] Health Protection Technology Division, ENEA-Casaccia, 00123 Rome, Italy

[2] Department of Biology, Tor Vergata University, Rome, Italy

[3] Danish Cancer Society Research Center, Copenhagen, Denmark

| | |
|---|---|
| PD | Parkinson's disease |
| PI | Propidium iodide |
| PMA | Phorbol 12-myristate 13-acetate |
| RA | Retinoic acid |
| RMS | Root-mean-square |
| ROS | Reactive oxygen species |
| SN | Substrantia nigra |

## Introduction

Parkinson's disease (PD) is a neurodegenerative disorder characterized by the progressive loss of dopaminergic (DAergic) neurons in the substrantia nigra (SN) pars compacta with a concomitant accumulation of intra-cytoplasmic neuronal inclusions (Lewy bodies, LBs) of α-synuclein [1].

The neurodegenerative mechanisms underlying PD have not yet been exhaustively elucidated, albeit, among the main responsible events for nigral neurons degeneration and death [2], current hypotheses include the following: (i) oxidative stress through mitochondrial dysfunction, (ii) accumulation of transition metals, (iii) dysfunction of protein folding quality control, (iv) inflammation and depletion of neurotrophic supports, and (v) deficits in antioxidant defense mechanisms. All these molecular defects are likely to cooperate in irreversibly damaging DAergic neurons in a complex molecular cross-talk leading to death [3].

Although free radicals are essential for physiological processes, especially in brain metabolism, the high metabolic rate and the polyunsaturated fatty acids-rich composition make this organ more sensitive to oxidative stress-driven degeneration [4]. Specific types of oxidative damage are indeed reported in the SN of PD patients, although they are not restricted to this brain region [5]. As the sources of the majority of energy production and endogenous ROS production, mitochondria play a key role in the functioning and survival of neurons in the brain, the most energy-intensive organ in the human body. The involvement of mitochondrial dysfunction as a causal factor of PD is well supported by observations in patients [2, 6]. Cysteine thiols and reduced glutathione (GSH) being the master redox buffers and cofactor in signal transduction, antioxidant and electrophile defense, dysregulation of their homeostasis is believed to contribute to initiation and progression of neurodegenerative diseases, including PD [7].

PD is thought to have a multifactorial etiology, frequently including both genetic and environmental factors [8, 9]. Epidemiologic and toxicological studies have shown that environmental agents, mainly pesticides and heavy metals, represent primary classes of neurotoxic agents associated with PD [10, 11]. More recently, several reports indicate that occupational exposure to electromagnetic fields might be associated with an increased risk of neurodegenerative diseases, mainly Alzheimer's disease (AD) and amyotrophic lateral sclerosis (ALS) [12–15]; however, the epidemiological evidence supporting an univocal association between PD and exposure to electromagnetic fields remains poor and controversial [15, 16]. In this context, ELF-MF (between 1 Hz up to 100 kHz, originating from power lines and household appliances, as well as welding machines, induction heaters, and transport systems) has been the factor generating most attention in neurodegenerative etiopathogenesis, as the interaction between ELF-MF and biological systems directly involves oxidative stress, in particular through the radical-based mechanism [17]. The molecular feature potentially associating ELF-MF with neurodegeneration relies on the redox imbalance which they trigger in brain [15, 18–21]. Despite this hypothesis, in vitro and in vivo experimental findings, which aim specifically at disclosing the potential PD/ELF-MF correlation, are still sparse and inadequate [15].

Our purpose was to assess whether exposure to ELF-MF might alter the response of the SH-SY5Y human neuroblastoma cell line to $MPP^+$ (1-methyl-4-phenylpyridinium), a specific in vitro PD model. Several neurotoxic chemicals are used to damage dopaminergic cells in vitro and in vivo and induce PD-like symptoms, mainly the synthetic compounds methyl-4-phenyl-1,2,3,6-tetrahydropyridine (MPTP) [22, 23]. MPTP induces Parkinsonism in humans and primates [24], via its active metabolite $MPP^+$ accumulating within the mitochondria, interferes with complex I of the electron transport chain, promotes the generation of reactive oxygen species (ROS), and eventually leads to neuronal cell death [23–25]. Here, we demonstrate that ELF-MF alters cellular redox homeostasis and thiol content in both proliferating and DA-differentiated SH-SY5Y cells, without affecting their growth and survival. We provide evidence that if administered before $MPP^+$ treatment, ELF-MF sensitize cells to $MPP^+$-induced toxicity through the induction of a massive oxidative stress and caspase-dependent apoptosis.

Taken as whole, our data attempt to provide a new perspective for interpreting the role of the environment in PD onset and focus on concern over exposure to EMFs as a potential environmental pollutant and novel risk factor in neurodegeneration.

## Materials and Methods

### Chemicals

Culture media, serum and supplements, trypsin-EDTA, phosphate buffer saline (PBS), and Hank's balanced salt solution (HBSS) were obtained from Euroclone (Milan, Italy). Hydrogen peroxide ($H_2O_2$), 1-methyl-4-phenylpyridinium iodide ($MPP^+$), all-trans retinoic acid (RA), phorbol 12-myristate 13-acetate (PMA), L-buthionine-sulfoximine (BSO), N-acetyl cysteine (NAC), ethylene-diamine-tetra-acetic acid (EDTA), glutathione ethyl ester (GSHest), dimethyl sulfoxide

(DMSO), RNAse A, Triton X-100, Trypan blue solution (0, 4 %), and Propidium Iodide (PI) were purchased from Sigma-Aldrich (Milan, Italy).

The fluorescent probes dihydroethidium (hydroethidine, DHE), 2′,7′-dichlorofluorescin diacetate ($H_2$-DCFDA), and CellTracker™ Green CMFDA (5-Chloromethylfluorescein Diacetate) were obtained from Molecular Probes (Life Technologies, Grand Island, NY, USA).

### Cell Culture and Differentiation

Human SH-SY5Y neuroblastoma cells were purchased from the European Collection of Cell Culture, cultured in complete Dulbecco's modified Eagle's medium/Ham's F12 (DMEM/F12 (50:50 mix, Euroclone), supplemented with 10 % heat-inactivated fetal bovine serum, 2 mM L-glutamine, 100 μg/ml penicillin-streptomycin, and kept in culture up to 15 passages. The cells were maintained at 37 °C in a 5 % $CO_2$ atmosphere in air and routinely trypsinized and plated at $4\times10^4/cm^2$ on flasks. Cell viability was assessed by Trypan blue dye exclusion.

At 60–70 % confluence, cells were sub-cultured and differentiated into a dopaminergic phenotype with 5 μM RA for the first 3 days, followed by 80 nM PMA for further 3 days in reduced serum condition (5 %) [26]. The dose of 5 μM RA was selected in the range between 1 and 10 μM as it allowed a detectable expression of dopamine transporter and tyrosine hydroxylase without severely affecting cell viability.

### Exposure System

The ELF-MF exposure system consists of two couples of square coils (two coils for each system) designed in Helmholtz configuration (Fig. 1a) [27]. This provides higher B-field levels with improved homogeneity. The coils have a side length (L) of 38 cm, and they are placed 12 cm apart (d) component, as shown in Fig. 1b. The coil section is square with a side of 2 cm (s) (Fig. 1b) and is composed of 25 cable turns. Each cable is made of copper with two wires with a diameter of 2.5 mm.

The coils are connected to a Variac (40NC) for voltage feeding and current circulation within the cable turns. The two systems are used for B-field and sham exposure of the biological samples at the same time, thus allowing blind experimental conditions. The coil double wire configuration is used for sham exposure implementation, which makes it possible to obtain a null B-field, using currents flowing in opposite directions [28]. In particular, sham samples are placed in the exposure system in the same position as the exposed ones. Each device is placed inside a standard incubator to ensure suitable environmental conditions for cell maintenance (Fig. 1a). In order to guarantee the temperature stability (37 °C) inside the incubators, a refrigerating system, consisting of water from two separate thermostatic baths and circulating in plastic tubes surrounding the coils, was set-up to prevent heating due to ohmic losses, thus maintaining the temperature of both B-field and sham-exposed samples at 37.0±0.2 °C. Temperature was monitored in the exposure volume of each incubator by two T-thermocouple probes (SENSORTEK Inc, Clifton, NJ, USA, placed in a dummy Petri dish and in air.

The B-field produced by these systems, at the operating frequency of 50 Hz, was set at 1 mT (RMS) for a supplied current of 3.4 A. The sham exposures were performed with a small residual B-field amplitude of about 0.3 μT (RMS), representing the background field emitted by the incubator electronics. B-field measurements in the center volume of the two coils arranged coaxially were performed with an isotropic probe (ELT400; Narda, Pfullingen, Germany) in both configurations. To define the B-field homogeneity within the

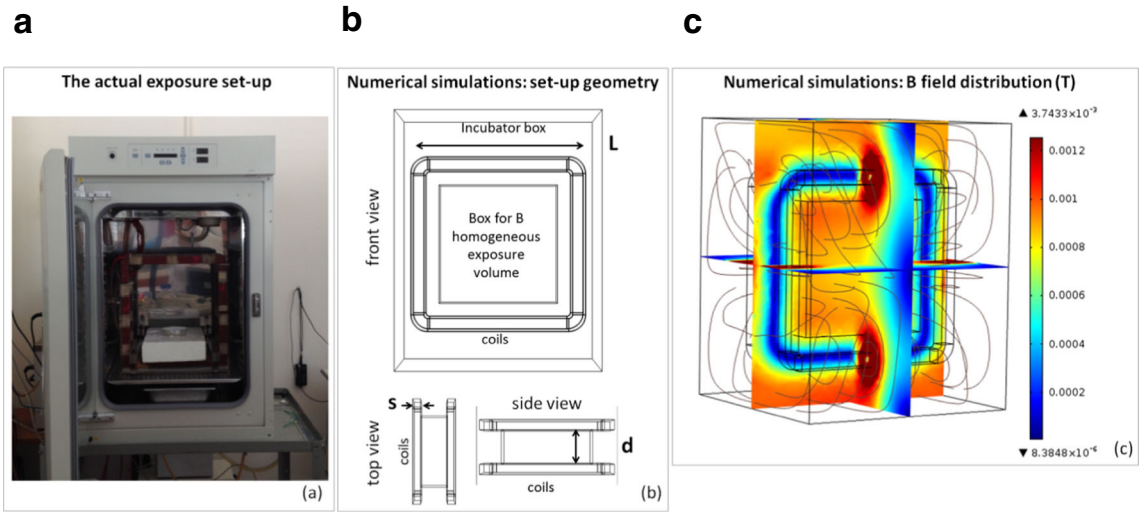


**Fig. 1** Representation of the ELF-MF exposure device and B field geometry. **a** The actual ELF exposure system placed inside the incubator is shown. **b** The exposure setup geometry used for electromagnetic simulations. **c** The B field distribution within the exposure setup is shown. The B field streamlines are visible in black, the computed mean B field values is 0.95 mT in optimum agreement with the measured field level

exposure setup and the induced E field values within the culture samples contained in Petri dishes, as recommended by Kuster and colleagues for high quality control of EMF exposure systems and protocols [29], numerical simulations were carried out. The exposure system was analyzed using finite element approach (Fig. 1b), and an equivalent current density distribution was used to supply the coils at 50 Hz.

Different sets of simulations were carried out, considering both the empty coils and with the biological samples contained in Petri dishes inside. In the empty structure, the B-field distribution and its homogeneity were evaluated, considering different exposure volumes. The variation coefficients (VC), defined as the ratio between the simulated standard deviation and the B field mean value, were computed inside the empty structure for different exposure volumes to arrange stacks of Petri dishes. Specifically, a good homogeneity level (VC=95 %) was observed for B-field in a large volume, $20\times20\times10$ cm$^3$ (Fig. 1c), thus making the system especially suitable for controlled exposures of a wide number of in vitro samples. Therefore, on the basis of simulation indications, the biological samples were placed within such an exposure volume. Then, the Petri dishes (60 mm) were simulated inside the coils. Each dish was filled with 4 mL of sample liquid comparable to the volume used during real cell culturing; a sample culture medium relative permittivity equal to 78 and an electric conductivity of 0.5 S/m at 50 Hz was used in simulations. The Petri dishes were positioned in two stacks of five containers each, and placed with their bottom layer parallel to the B-field direction (B-field streamlines visible in Fig. 1c). The induced E-field distribution was evaluated together with the homogeneity level within each Petri dish and in the whole culture medium volume. Results showed that the biological samples were exposed to an induced E-field of low intensity, nearly 0.5 mV/m (RMS) with a homogeneity of about 95 % for adherent cells at the bottom layer of the dish.

Globally, our experimental and numerical data guaranteed proper positioning of the biological samples throughout all the experiments and under rigorously controlled and repeatable exposure conditions.

### ELF Exposure and Cell Treatments

For ELF-MF exposure (50 Hz, 1 mT), cells were seeded in 60-mm Petri dishes and placed in either ELF-MF or sham incubator (under blind condition) 24 h after plating. Cells underwent a continuous exposure to ELF-MF/sham over a time window of 6–72 h. $MPP^+$ stock (100 mM in DMSO) was diluted to reach 0.1 to 5-mM concentrations in complete medium before each single experiment. In both proliferating and differentiated conditions, $MPP^+$ was administered after 24 h of sham/ELF-MF exposure and left in the medium for further 6–24 h until analyses. Over treatment with $MPP^+$, the exposure system was kept switched-off. For the recovery experiments, $MPP^+$ was removed from the cell media, and replaced with fresh complete medium.

BSO, NAC, and GSHest were dissolved in PBS to 100-mM stock and filtered, then diluted with serum-free DMEM/F12 medium to final concentrations and maintained throughout the experiment. Since GSH solution is highly acidic, pH was adjusted with 7.5 % $NaHCO_3$. BSO was added 24 h prior to $MPP^+$ administration, whereas GSHest and NAC 6 h before.

### Flow Cytometric Analysis

A FACScan flow cytometer (Becton Dickinson, Bedford, MA, USA) equipped with a 488-nm argon laser was used for the flow-cytometric analysis. Forward (FSC-H) and side scatters (SSC-H) were used to establish size and granularity parameters, respectively, and to exclude cellular debris from the analysis, in order to delimitate the integer/healthy cells gate (defined $R_1$). Only cells contained in the $R_1$ region were included in the fluorescence analysis.

The excitation wavelength was set at 488 nm. The observation wavelength of 530 nm was chosen for green fluorescence and 585 nm for red fluorescence, and the intensities of emitted fluorescence were collected on FL1 and FL2/3 channels, respectively. In each measurement, a minimum of 10,000 cells were analyzed. Data were acquired and analyzed using the Cell Quest software (Becton Dickinson). For fluorescence data analysis, the mean fluorescence intensity (MFI) was calculated for each sample as the ratio between the mean fluorescence value in the channel of the probe-labeled cells versus the unstained ones (negative).

**Determination of ROS** To quantify ROS generation, cells were stained with DHE and $H_2$–DCFDA in order to detect superoxide and $H_2O_2$, respectively. Cells were quickly scraped on ice, washed twice in cold PBS, and re-suspended in either 5 μM DHE (20′, 37 °C in the dark, in PBS) or 5 μM $H_2$DCFDA (30′, 37 °C in the dark, in HBSS). After a final wash in PBS, cells were immediately transferred into a tube on ice for flow cytofluorometric analysis [30, 31].

**Detection of the Cellular Thiol Content** CellTracker™ Green CMFDA was dissolved in DMSO (1:100 *v*/*v*), and stored at 4 °C in the dark. Cells were stained in complete medium with 1 μM CMFDA at 37 °C, 10′, in the dark, washed in PBS and transferred into a tube on ice for flow cytofluorometric analysis [32].

**Apoptosis Assessment** Apoptosis was evaluated by either Annexin V/PI double staining (FITC Annexin V/Dead Cell Apoptosis kit, Molecular Probes) or by propidium iodide (PI) staining performed upon ethanol fixation [33].

For annexin labeling, cells were simultaneously incubated with the Annexin-V-FITC and PI, according to the

manufacturer's instructions. Propidium iodide-negative cells, displaying a positive fluorescence for the Annexin V-FITC staining, were gated and considered as apoptotic ($AnnV^+/PI^-$). Treatment with staurosporine (1 μM, 24 h) was used as positive control for condition setup and gating. The Annexin $V^+/PI^+$ cells are recorded as very late apoptotic/necrotic and have been excluded from the analysis [34].

The determination of hypodiploid (Sub-$G_1$, apoptotic) nuclei was carried out by staining fixed cells with PI (50 μg/ml) in a mix containing RNAse A (50 μg/ml), Triton X-100 (0.1 %), and EDTA (0.1 mM) in PBS, in the dark, for 60 min at room temperature.

**Caspase Cleavage** Caspase activation was assessed by the CellEvent™ Caspase-3/7 Green Detection kit (Molecular Probes), according to manufacturer's instruction. Briefly, $1 \times 10^5$ cells were labeled with 5 μM of the detection reagent (freshly diluted) in complete medium, for 30 min, at room temperature in the dark, counterstained with PI (10 μg/ml), and immediately analyzed by flow cytometry. As the green dye emits fluorescence only if cleaved by the active caspase-3/7, the percentage of CellEvent™-$^+/PI^-$ cells were gated and recorded as active caspase-3/7-containing cells [35]. Treatment with staurosporine (1 μM, 24 h) was used as positive control for condition setup and gating.

## Western Blotting

Cells were resuspended in lysis buffer containing 50 mM Tris-HCl (pH 8.0), 150 mM NaCl, 1 % NP-40, and 12 mM Na-deoxycholate (Sigma) supplemented with protease and phosphatase inhibitors cocktail (Merck, Germany). Lysates were centrifuged at 13,000 rpm for 10 min at 4 °C to discard cellular debris. Protein concentration was determined by the Lowry protein assay (Bio-Rad Laboratories, Hercules, CA, USA). Proteins were separated by SDS-PAGE and transferred to nitrocellulose membranes (GE Healthcare Life Science, Europe) that were probed with the following antibodies: anti-PARP1, anti-tubulin (SIGMA), and anti-actin (Santa Cruz). After immuno-staining with appropriate secondary horseradish peroxidase-conjugated goat anti-rabbit or anti-mouse antibodies (SIGMA), bands were revealed by a Fluorchem Imaging system (Alpha Innotech, San Leandro, CA, USA), using the Amersham ECL detection system (GE Healthcare Life Science) and quantified by densitometry.

**Protein Carbonylation** Carbonylated proteins were detected using the Oxyblot Kit (Intergen, Purchase, NY) after reaction with 2.4-dinitrophenylhydrazine (DNP) for 15 min at 25 °C. Samples were then resolved by 10 % sodium dodecyl sulfate polyacrylamide gel electrophoresis (SDS-PAGE), and DNP-derivatized proteins were identified by immunoblot using an anti-DNP antibody [31].

## Statistical Analysis

All data are expressed as mean±SD calculated in $N \geq 3$ replicates. Statistical analyses were performed using the non-parametric two-way ANOVA-Friedman test. $P$ values <0.05 were considered statistically significant.

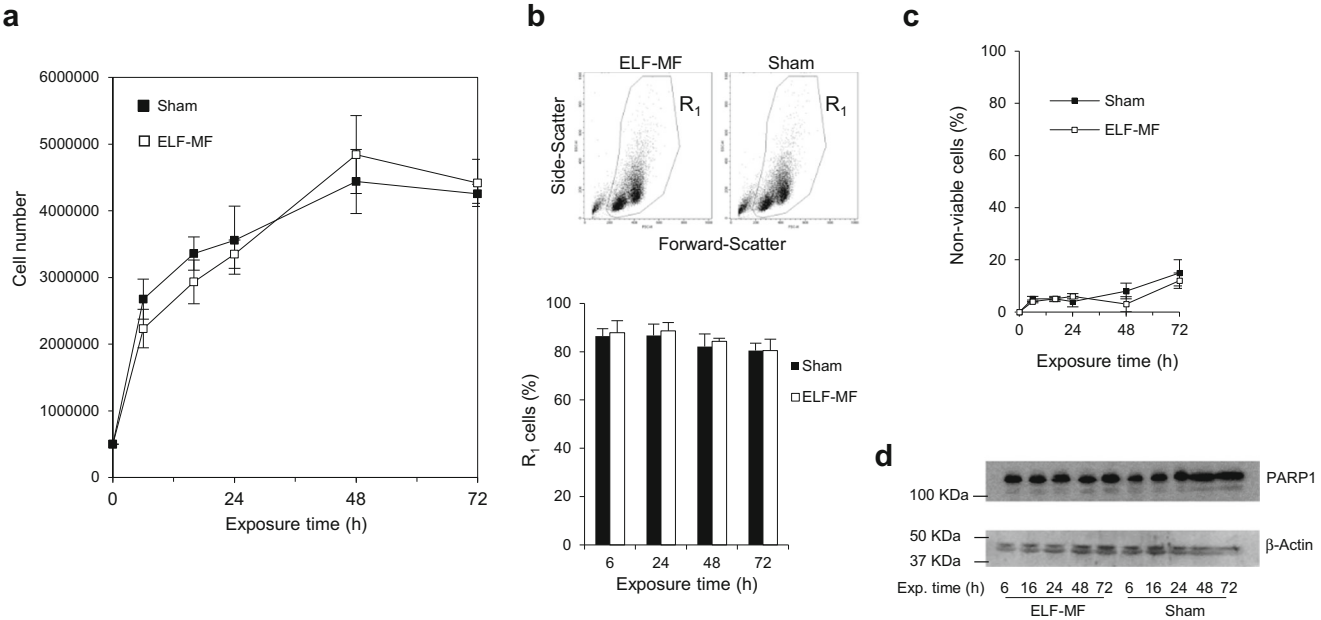


**Fig. 2** ELF-MF exposure does not affect proliferation, morphology, and viability of proliferating SH-SY5Y cells. Evaluation of **a** cell growth, **b** size/morphology performed by flow cytometry (FSC-H vs SSC-H), **c** viability (Trypan blue exclusion), and **d** apoptosis by PARP1 cleavage (molecular masses are given in kDa on the left), carried out in proliferating SH-SY5Y cells following 6–72 h of continuous exposure to either ELF-MF or sham. Values are means±SD ($N$=7). The immunoblot is a representative of different experiments giving similar results

## Results

**Exposure to ELF-MF Alters Redox Homeostasis and Leads to Protein Carbonylation in SH-SY5Y Cells** We first characterized the biological response of proliferating SH-SY5Y dopaminergic cells to the ELF-MF (50 Hz continuous wave frequency, 1 mT RMS amplitude), over a time window of 6–72 h of continuous exposure. The characteristics of the exposure setup and electromagnetic field geometry are described in detail in Fig. 1. As reported in Fig. 2a–c, exposure to ELF-MF did not induce any phenotypic change in terms of growth, cell morphology/size, and viability. Moreover, no apoptosis activation was observed in cells upon ELF-MF or sham exposure, as demonstrated by the absence of PARP1 cleavage (Fig. 2d).

ELF-MF has been reported to affect redox state in brain [15, 18–21]. Therefore, to verify whether the presence of ELF-MF might trigger ROS generation also in our experimental model, we measured superoxide and hydrogen peroxide by both DHE (dihydroethidium) and $H_2$-DCFDA (2′,7′-dichlorofluorescein diacetate) staining, respectively. Results shown in Fig. 3a–b clearly indicate that, at each time point analyzed, ELF-MF exposure induced a small but

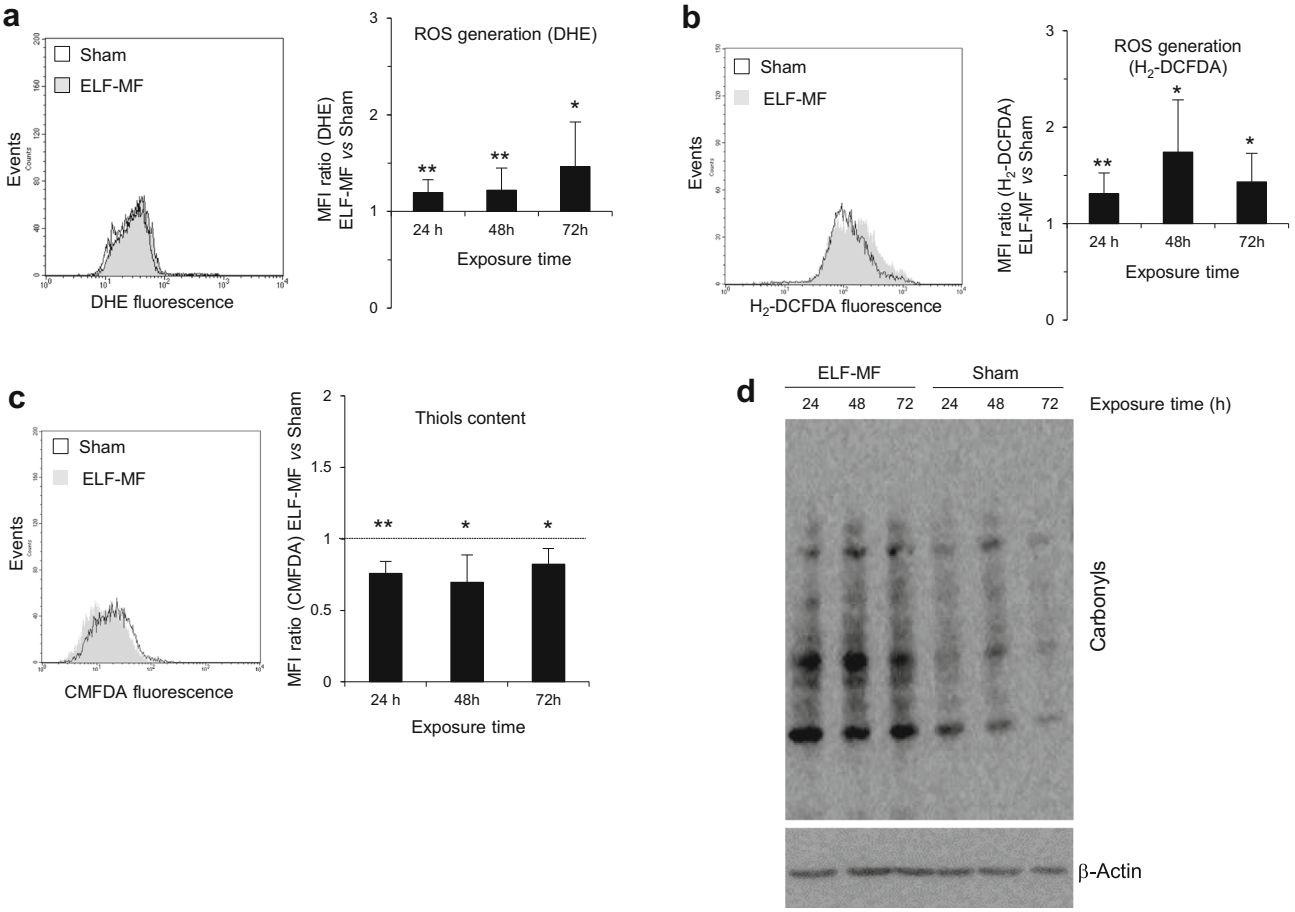


**Fig. 3** ELF-MF exposure alters the redox balance and induces protein carbonylation in proliferating SH-SY5Y cells. Flow cytometric analysis of ROS generation carried out by **a** DHE (5 μM in PBS, 20′, 37 °C in the dark) and **b** $H_2$-DCFDA (5 μM in HBSS, 30′, 37 °C in the dark) viable labeling. **c** Evaluation of intracellular content of thiols performed by CMFDA labeling (1 μM in PBS, 37 °C, 10′, in the dark). Data are expressed as the ratio of the mean fluorescence intensity (MFI) calculated in the ELF vs Sham-exposed cells. **d** Immunoblot analysis of total protein carbonylation (Oxyblot Kit). All the evaluations have been carried out at 24, 48, and 72 h of continuous ELF-MF/sham treatment. Values are means±SD ($N$=4). *$P$<0.05, **$P$<0.01 calculated in ELF-MF vs sham-exposed cells. Immunoblot and FACS plots reported in the figure are each from a typical experiment representative of four others giving similar results

**Fig. 4** ELF-MF exposure increases the susceptibility to the $MPP^+$ toxin. Analysis of the relative proliferation index and viability (Trypan blue exclusion) carried out in proliferating SH-SY5Y cells undergoing **a** ELF-MF/sham exposure plus $MPP^+$ treatment (ranging from 0.1 to 2.5 mM for 24 h), and **b** same schedule as in **a** followed by 24 h of recovery in fresh medium. Evaluation of apoptosis carried out by **c** Annexin V/PI staining, **d** immunoblot of PARP1 cleavage, and **e** caspase 3/7 activation, in cells undergoing ELF/sham plus $MPP^+$ treatment (indicated doses, 24 h). In the representative FACS dot plots reported in the figure (out of three other experiments leading to similar results), apoptotic cells are referred as the Annexin $V^+/PI^-$ (highlighted in the box with percentage) also displaying a positive labeling for casapse3/7 specific probe (shown in the box with relative percentage). Values are means±SD ($N$=3). *$P$<0.05, **$P$<0.01 calculated in ELF-MF vs sham-exposed cells

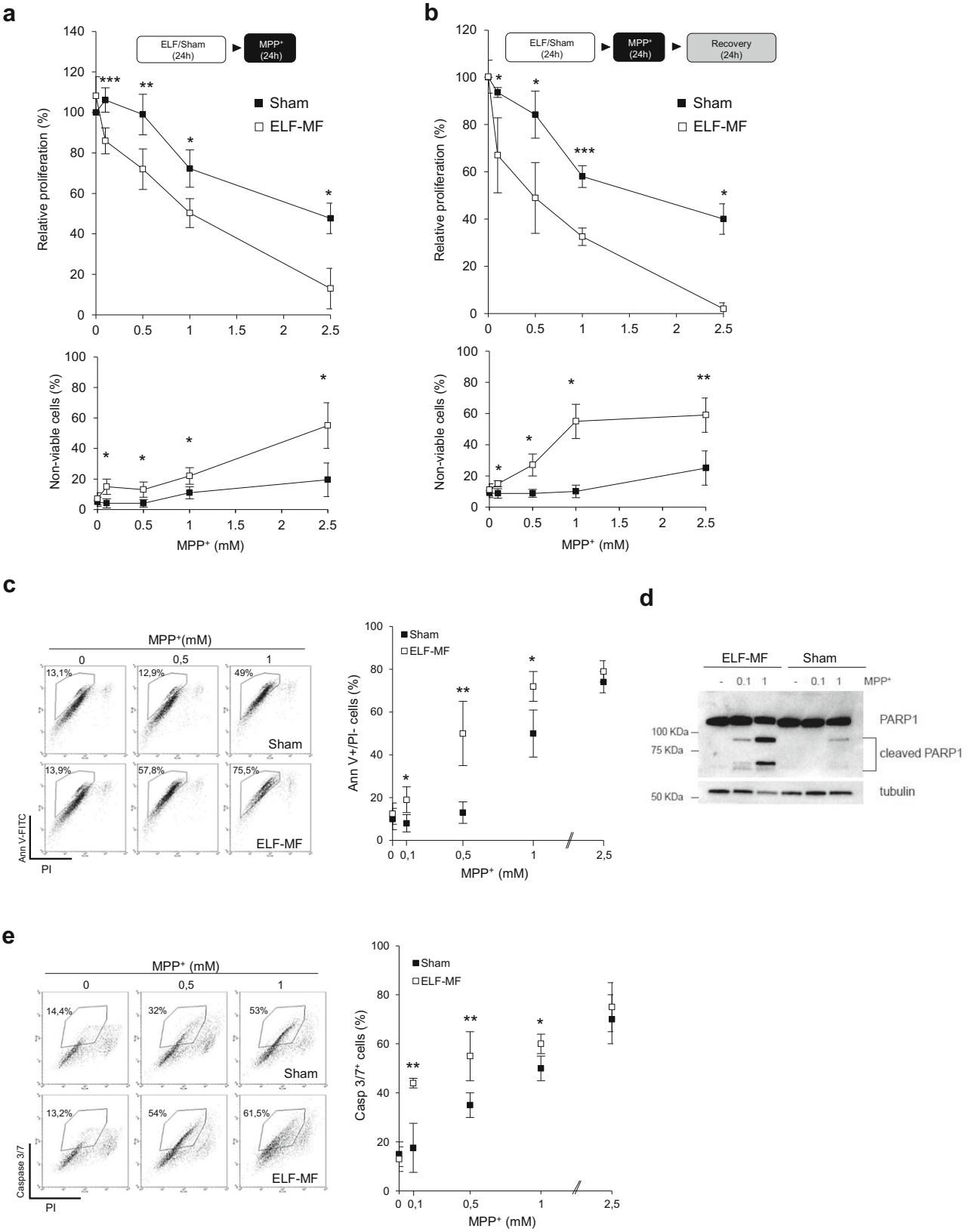


significant increment in ROS production with respect to the sham-exposed counterpart. In line with this, we observed a concomitant depletion in the intracellular thiol pool whose measurement has been carried out by the use of CMFDA (5-chloromethylfluorescein diacetate), a probe reacting with free sulfhydryls, such as GSH, which represents the main

intracellular thiol acting as ROS scavenger [32]. Figure 3c shows that CMFDA fluorescence significantly and irreversibly decreased in SH-SY5Y dopaminergic after exposure to ELF-MF. Moreover, under these experimental conditions, SH-SY5Y cells displayed a clear and massive increase in total protein carbonylation (Fig. 3d), a covalent irreversible post-translational modification used as specific biomarker of oxidative damage [36].

**ELF-MF Exposure Sensitizes SH-SY5Y Cells to $MPP^+$ Challenge** SH-SY5Y cells mimic many aspects of the DAergic neuron death observed in PD when treated with neurotoxins such as $MPP^+$ [37, 38]. In accordance with previous reports, we verified that $MPP^+$ treatment was able to trigger SH-SY5Y cell death via the activation of caspase 3/7, the induction of p53 and downstream gene expression (e.g., p21/puma/bax), and the generation of ROS in a dose-dependent manner (0.1–5 mM range) (Online Resource 1).

On the basis of these results, we used $MPP^+$ in combination with ELF-MF in order to verify whether the ELF-MF-driven redox imbalance might alter SH-SY5Y cell response profile to $MPP^+$. The administration schedule consisted in 24 h of continuous ELF-MF exposure, followed by 6-to-24 h treatment with $MPP^+$. As reported in Fig. 4a, growth inhibitory and cytotoxic effects elicited by $MPP^+$ were significantly potentiated when cells were pre-exposed to ELF-MF. This phenomenon was particularly evident at low doses of $MPP^+$ (0.1 mM), and even more sustained in the recovery experiments (Fig. 4b), indicating that the ELF-MF-induced oxidative stress irreversibly primed the cells to cell death induced by $MPP^+$.

**Fig. 6** ELF-MF potentiates the $MPP^+$ toxicity in differentiated SH-SY5Y. **a** Proliferative response to different doses of RA/PMA combination treatment in the SH-SY5Y cells. **b** Schematic description of the administration schedule applied to cells for RA/PMA differentiation and combined ELF/$MPP^+$ treatment. Evaluation of **c** cell growth, **d** size/morphology by FACS analysis, **e** viability (trypan blue exclusion), and **f** ROS generation/thiol content carried out by FACS assessment in the differentiated SH-SY5Y cells following 24–72 h of continuous exposure to either ELF-MF or sham. Assessment of apoptosis occurring in differentiated SH-SY5Y cells, following ELF/sham exposure (24 h) plus $MPP^+$ treatment, by means of **g** Annexin V/PI viable staining, caspase-3/7 activation, and **h** analysis of the sub-$G_1$ (pyknotic nuclei) percentage by flow cytometry. Values are means± SD ($N$=3). *$P$<0.05, **$P$<0.01 calculated in ELF-MF vs sham-exposed cells. PI plots reported represent a typical experiment out of three leading to similar results

At the molecular level, we observed that ELF-MF-induced enhancement of $MPP^+$ toxicity was due to an increased rate of apoptosis. Indeed, at any dose of $MPP^+$ employed, the percentage of annexin $V^+/PI^-$ (apoptotic) cells was higher in SH-SY5Y cells pre-exposed to ELF-MF with respect to the sham control (Fig. 4c). These results were consistent with those obtained upon Western blot analyses of PARP1 cleavage (Fig. 4d), and coherent with the percentage of caspase-3/7-activating cells, which was higher if cells were pre-exposed to ELF-MF (Fig. 4e). However, any differences was lost when higher $MPP^+$ concentration (2.5 mM) was administered to the cells, indicating that, in these conditions, there was no further modulation of $MPP^+$ toxicity.

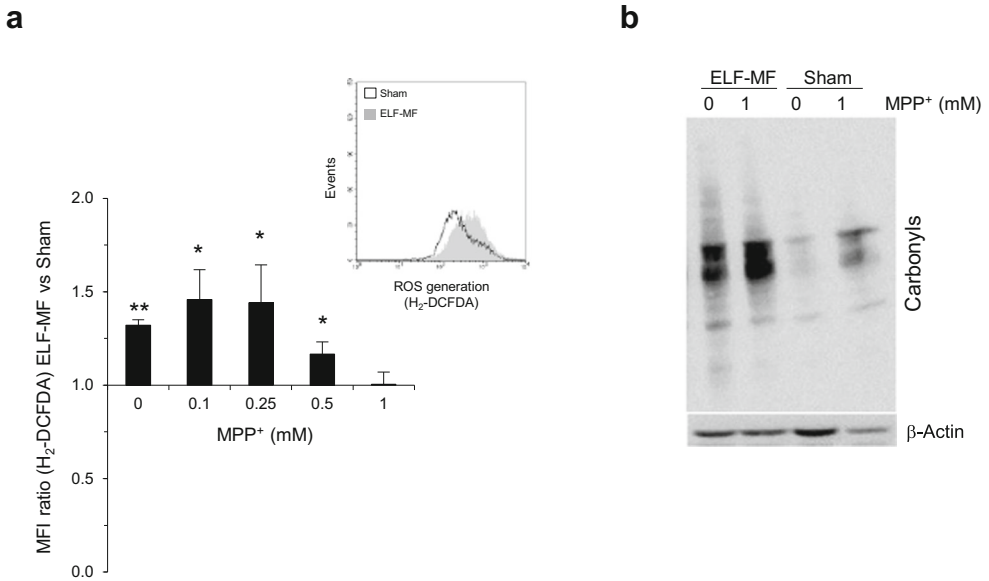


**Fig. 5** ELF-MF-induced enhancement of $MPP^+$ toxicity is associated with an increased oxidative stress. **a** Evaluation of ROS generation carried out in cells, treated with the indicated doses of $MPP^+$, by $H_2$-DCFDA viable labeling and FACS analysis. The data are presented as MFI ratio of ELF-MF vs sham. Values are means±SD ($N$=4, *$P$<0.05). The $H_2$-DCFDA fluorescence figure is a representative mono-parametric diagram out four different experiments with similar results. **b** Protein carbonylation analysis performed in the ELF/sham exposed cells, undergoing treatment with 1 mM of $MPP^+$ drug. The immunoblot is a representative of different experiments giving similar results

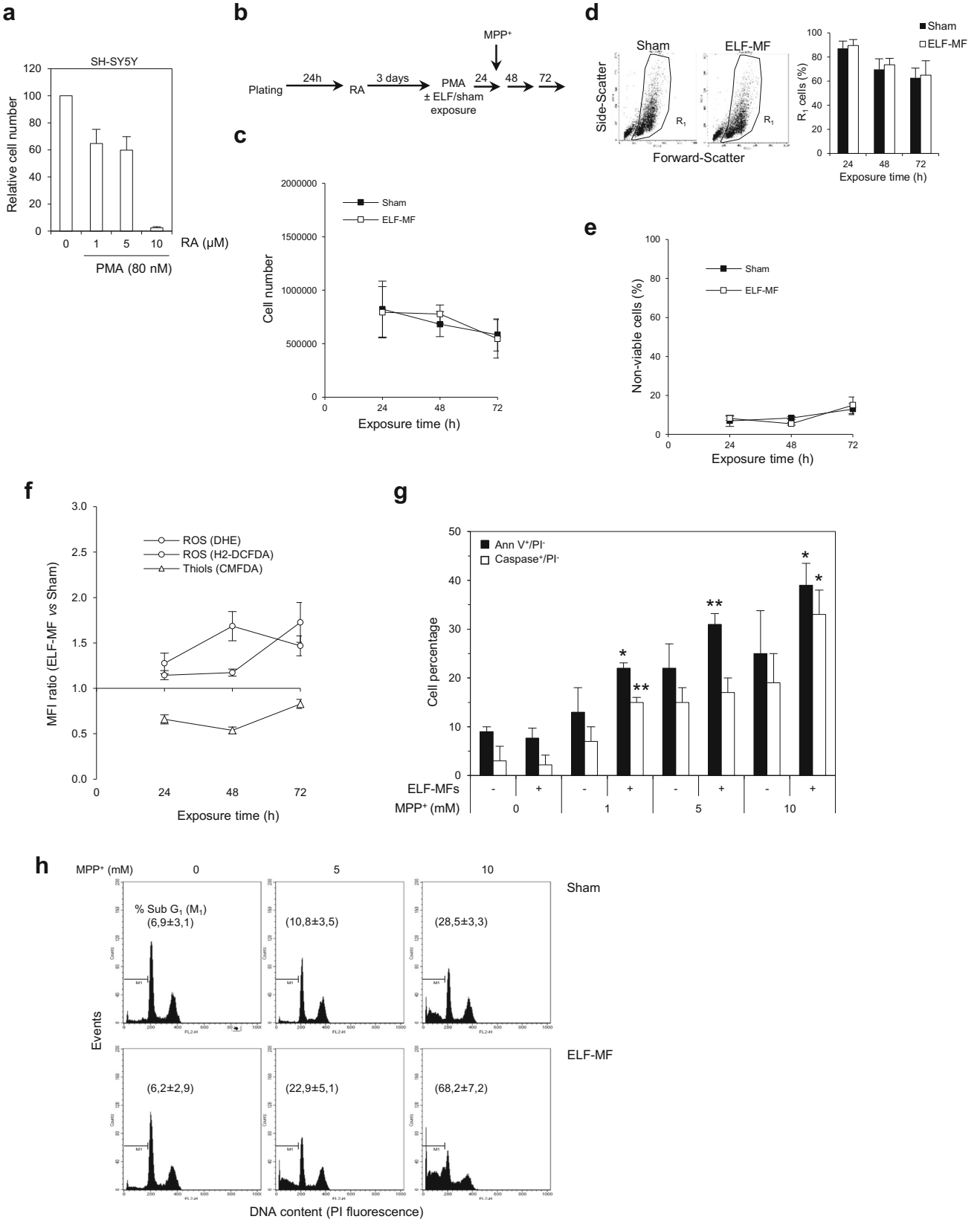


**ELF-MF-Induced Enhancement of MPP$^+$ Toxicity is Associated with an Increased Oxidative Stress** We previously demonstrated that ELF-MF exposure affects intracellular redox state. Therefore, in order to understand whether ELF-MF-

mediated potentiation of $MPP^+$ toxicity was related to oxidative conditions, we analyzed ROS production and protein carbonylation. Results shown in Fig. 5a indicate that ELF-MF pre-exposure induced a significant increase of ROS levels with respect to the sham-exposed control. In line with this evidence, the combined treatment (ELF-MF plus $MPP^+$) resulted in a further increase of protein carbonylation, when compared to ELF or to $MPP^+$ alone (Fig. 5b).

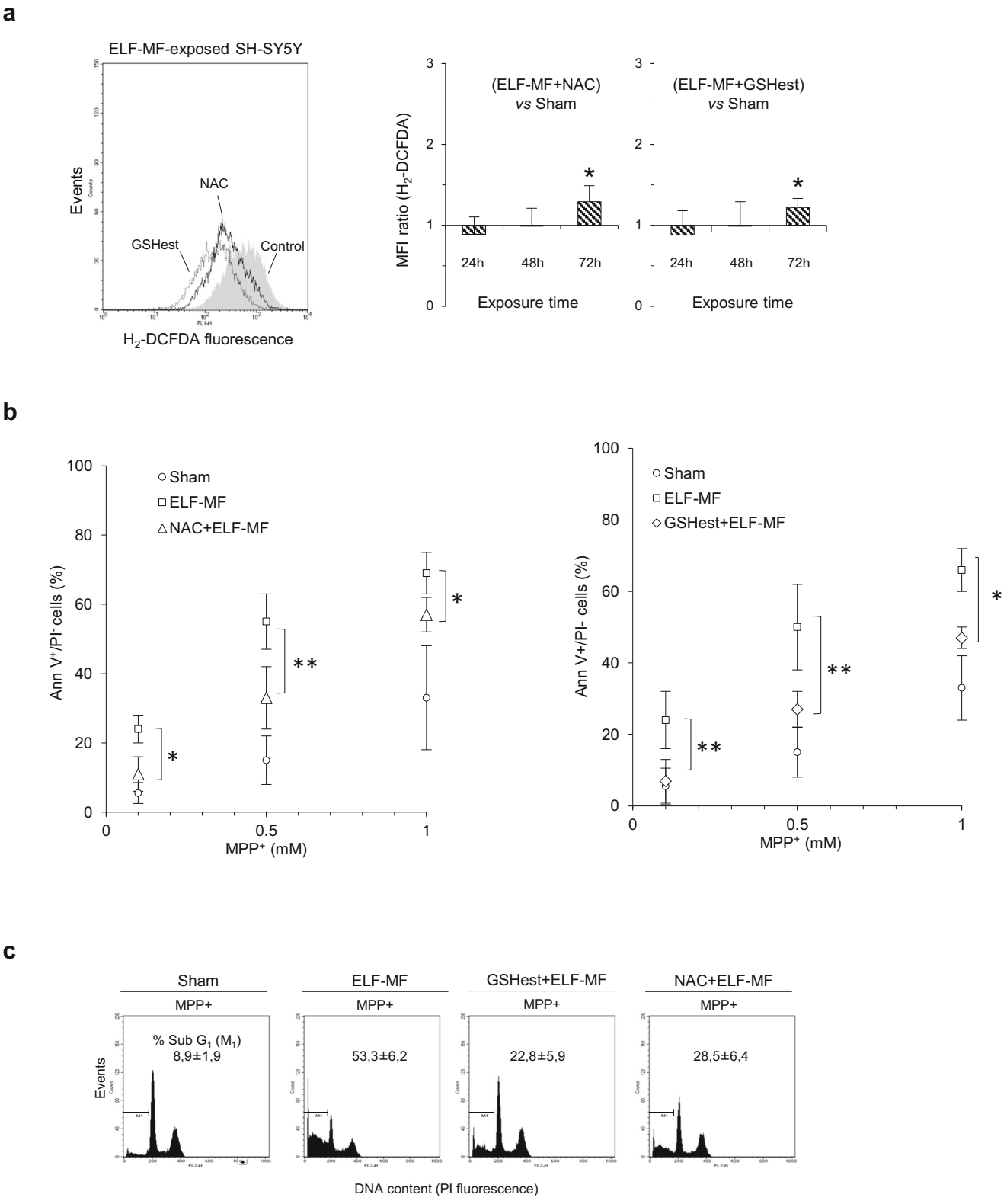

◀ **Fig. 7** Thiol redox state imbalance contributes to ELF-MF-induced sensitivity to $MPP^+$. Either NAC (1 mM) or GSHest (1 mM) have been added to culture media 6 h before ELF/sham switching-on. After 24 h of continuous exposure, cells have been given $MPP^+$ for 6–24 h and immediately analyzed by flow cytometry. **a** Evaluation of ROS generation performed by $H_2$-DCFDA viable labeling at 24, 48, and 72 h of continuous ELF/sham exposure. The FACS plot (left) represents the $H_2$-DCFDA fluorescence after 24 h of ELF-MF exposure, and is a typical one out of three experiments with similar results. The histograms (*right*) show the $H_2$-DCFDA MFI ratio calculated in the NAC/GSHest-ELF vs sham. Values are means±SD ($N$=3, *$P$<0.05). Assessment of the $MPP^+$-induced apoptosis carried out by **b** Annexin V/PI staining of viable cells, and **c** evaluation of the sub-$G_1$ population with pyknotic nuclei, carried out by flow cytometry in cells treated with the indicated doses of $MPP^+$ for 6 h (**b**) and 24 h (**c**). Values are means±SD ($N$=3). *$P$<0.05, **$P$<0.01 calculated in the NAC/GSH-ELF-MF cells vs ELF-MF counterpart. PI histograms reported are from one typical experiment out of three leading to similar results

**ELF-MF is Able to Potentiate $MPP^+$ Toxicity in Differentiated SH-SY5Y** In order to extend our results and to better mimic physiological conditions, we differentiated SH-SY5Y cells by sequential incubations with retinoic acid (RA) (5 μM, 3 days) and phorbol 12-myristate 13-acetate (PMA) (80 nM, 3 days) [26, 37, 38], and then subjected the cells to ELF-MF exposure (Fig. 6a). This dose/time combination was chosen in order to obtain a DAergic phenotype by stimulating the expression of dopamine transporter and tyrosine hydroxylase [26, 38, 39], without severely affecting cell viability (Fig. 6b).

Exposure of differentiated SH-SY5Y to ELF-MF displayed no difference with respect to the sham-exposed control in growth rate, size/morphology, and viability (Fig. 6c–e). Conversely, we observed an increase in both DHE and $H_2$-DCFDA fluorescence, together with a decline in the thiol content (Fig. 6f). As previously observed, we verified that this condition prepared the way for potentiating $MPP^+$ toxicity. However, at variance with proliferating SH-SY5Y, higher range of doses should be used in differentiated cells to trigger apoptosis via the activation of caspase3/7 (Fig. 6g). Matching these lines of evidence, we also observed a significant increase in the percentage of sub-$G_1$ (apoptotic) population after 24 h treatment with 5 and 10 mM $MPP^+$ (Fig. 6h). In particular, cytofluorometric analyses upon nuclear staining with propidium iodide highlight the higher sensitivity of differentiated SH-SY5Y pre-exposed to ELF-MF with respect to the sham-exposed control, confirming that ELF-MF sensitized dopaminergic neuronal cells to $MPP^+$ toxicity.

**Thiol Redox State Imbalance Contributes to ELF-MF-Induced Sensitivity to $MPP^+$** In order to confirm the pivotal role of oxidative stress as triggering event induced by ELF-MF and underlying susceptibility of SH-SY5Y to $MPP^+$, we modulated the intracellular thiol pool and analyzed any change in cellular response. As expected, inhibition of GSH de novo synthesis by 24-h incubation with 0.1–5 mM buthionine-sulfoximine (BSO) enhanced $MPP^+$ toxic effects in SH-SY5Y pre-exposed to ELF-MF, with cell growth rate reduced and the amount of non-viable cells increased in a dose-dependent manner (Online Resource 2a). This evidence was consistent with the positive shift in the $H_2$-DCFDA fluorescence (Online Resource 2b) observed upon BSO incubation.

We next evaluated whether the addition of the permeable thiol-based antioxidants NAC (*N*-acetyl-L-cysteine) or the ethyl ester form of GSH (GSHest) could counteract ELF-MF-induced enhancement of $MPP^+$ toxicity. As shown in Fig. 7a, both NAC and GSHest efficiently scavenged ROS, restoring the levels measured in the sham-exposed cells (Fig. 7a, right panels).

Consistently, NAC and GSHest were able to reduce the extent of $MPP^+$-induced apoptosis in ELF-MFs pre-exposed SH-SY5Y either if assessed by Annexin $V^+/PI^-$ (Fig. 7b), or propidium iodide staining (Fig. 7c), confirming the primary role of intracellular thiols in protecting neuronal cells to oxidative stress.

## Discussion

The last few years have seen increasing public concern about the health effects of both residential and occupational exposure to ELF-MF, such as those generated by high-tension electrical distribution networks, and typically affecting specific categories of workers (electric power installers and repairers, telephone line technicians and welders). Several studies have suggested a possible association of ELF-MF with neoplastic malignancies in childhood, as well as with diseases affecting the nervous system [40, 41]. In particular, ELF-MF has been associated with neurodegenerative diseases such as AD and ALS [12–15]. Epidemiological data have also highlighted the potential impact of ELF-MF exposure in brain and PD onset [15, 16], although evidence is still poor and controversial. This scarcity of evidence could be due to various reasons, such as limited statistical power found in most studies and, most of all, the wide variability of ELF-MF exposure levels between individuals enrolled in the studies, in terms of both time and intensity [15]. A convincing mechanism responsible for the pathological effects elicited by ELF-MF in brain is also lacking, although cell cycle/death impairment, protein modification, and, mainly, oxidative stress have been proposed as playing a crucial role [15, 39]. Several in vitro and in vivo findings have indeed demonstrated the occurrence of oxidative damage in neuronal cells following ELF-MF exposure [15, 18–21, 42]. All these lines of evidence support the hypothesis based on the "radical pair system" according to which ELF-MF contribute to prolonging the lifetime of free radicals and increasing their concentration in living cells [15, 17].

In this study, we aimed to provide clear-cut evidence for a detrimental role of ELF-MF in PD etiology based on their capability of generating basal oxidative stress conditions. In order to

understand the harmful effects of continuous exposure to ELF-MF, as well as their implication in contributing to PD onset and severity, we used a well-characterized dopaminergic cellular model (SH-SY5Y) [26, 37–41, 43, 44], and developed reliable and straightforward experimental conditions mainly in terms of electromagnetic requirements. To this end, device setup was conceived for three reasons: (i) to better reproduce an average environmental prolonged exposure to ELF-MF, selecting values of 1 mT, 50 Hz. This exposure represents the reference levels for occupational exposure set at 50 Hz by the ICNIRP (International Commission on Non-Ionizing Radiation Protection) [45], with an induced E-field value approximately a hundred times lower than the basic restriction for Central Nervous System occupational exposure [45]; (ii) to provide a very high homogeneity of the ELF-MF applied to the cells; and, in turn, (iii) to ensure a high reproducibility and quality of the results.

Results obtained in this study argue for prolonged ELF-MF exposure being unable per se to affect proliferation, viability, size, and morphology of both proliferating and differentiated SH-SY5Y cells. These observations are in agreement with Reale et al. who previously reported no impact in cell morphology and viability after 6–24 h of ELF-MF challenge in the same experimental model [46]. However, despite its inability to macroscopically affect cell phenotype and survival, we demonstrated that ELF-MF significantly affect redox homeostasis. This observation confirms evidence previously obtained in the same cell system and in other neuronal models [18–21, 42, 46, 47] and at the same time strengthens the hypothesis that oxidative stress plays a causative role in dopaminergic neuron dysfunction.

There is an open and unsolved debate regarding the upstream chemical process responsible for converting the ELF-MFs stimulus into an intracellular pro-oxidant event. This is particularly relevant in a dopaminergic cell context where dopamine metabolism implies side oxygen free radical production [48], and where deleterious activity of neurotoxins, inducing loss of DAergic neuronal population (e.g., rotenone and MPTP), mostly depends on their ability to target mitochondria and produce oxidative stress [49].

Although we still do not know how oxidative stress takes place, the observation that thiol pool decreases upon ELF-MF exposure argues for an impairment of the antioxidant defense being also crucial. We demonstrated that the modulation of GSH levels deeply affects the response to $MPP^+$, as the inhibition of GSH de novo synthesis by BSO exacerbates cell viability. In accordance, the replenishment of GSH intracellular content allows cell viability recovery. These results are in line with data from the literature reporting that GSH levels decrease both in SHSY5Y cells undergoing combined treatment ELF-MF/menadione [38], and in a number of PD models and human SN lesions [7, 50]. For instance, in incidental LBs disease, which may be considered a pre-symptomatic form of PD, GSH depletion is already present in the SN, and precedes complex I dysfunctions, iron accumulation, and striatal DA loss [51, 52], thus suggesting that GSH decreased levels could be an early event in PD etiology. Accordingly, NAC administration has been tested in animal models and clinical trials of PD [53, 54], and BSO has been already reported to significantly amplify in vivo (namely in nigral neurons) the toxic effects induced by MPTP [55]. Altogether, these pieces of evidence argue for thiol homeostasis being crucial for sustaining the antioxidant defense of DAergic neuronal cells and, in turn, for protecting them against irreversible oxidative damage. In support of this, different in vitro and in vivo studies demonstrated that GSH depletion triggers extensive carbonylation of brain proteins and morphological changes of DAergic neurons in the nigro-striatal pathway [52, 56, 57]. Here, we have provided evidence that ELF-MF exposure causes per se an increase of protein carbonyl content along with a decrement of the intracellular thiol pool. Overall, these observations suggest that ELF-MFs can induce PD-like conditions, thereby predisposing dopaminergic-like cells to be more vulnerable to $MPP^+$-induced challenge [22, 23, 36]. As a direct consequence, ELF-MF in combination with $MPP^+$ further pushes up the amount of total protein carbonylation and induces DAergic cell to death by a caspase-dependent apoptosis. Future experiments are required to identify whether key PD proteins, e.g., Parkin or α-synuclein, can undergo carbonylation upon ELF-MF-induced oxidative stress and whether this modification can induce a loss of function (e.g., by aggregation or degradation), which might be related to PD onset.

A number of reports suggest that calcium signaling and, most of all, changes in the gene expression profiling are also induced upon ELF-MF exposure [58, 59]. Based on these assumptions, we are currently evaluating the role of DNA methylation and microRNAs expression in response to ELF-MF exposure, and how these epigenetic effectors might interact with oxidative stress to affect/concur to $MPP^+$ toxicity. This would hopefully provide novel insights into the complex network of molecular processes finely tuned by life-long ELF-MF exposure and possibly contributing to PD onset.

**Acknowledgments** G.F. is supported by grants from the National Ministry of Health, Young Italian Researcher Grant-2008 (Grant GR-2008-1138121), and from the Italian Association for Cancer Research, AIRC-MFAG 2011 (Grant 11452). We are very grateful to Francesca Pacchierotti for her helpful criticisms and scientific support and to Martin W. Bennett for manuscript editing.

**Conflict of Interest** The authors declare no conflict of interest.

## References

1. Dauer W, Przedborski S (2003) Parkinson's disease: mechanisms and models. Neuron 39:889–909, **Review**
2. Thomas B, Beal MF (2007) Parkinson's disease. Hum Mol Genet 16:R183–R194
3. Binukumar BK, Bal A, Kandimalla RJ, Gill KD (2010) Nigrostriatal neuronal death following chronic dichlorvos exposure: crosstalk

between mitochondrial impairments, α synuclein aggregation, oxidative damage and behavioral changes. Mol Brain 3:35
4. Evans PH (1993) Free radicals in brain metabolism and pathology. Br Med Bull 49(3):577–587, **Review**
5. Alam ZI, Jenner A, Daniel SE, Lees AJ, Cairns N, Marsden CD, Jenner P, Halliwell B (1997) Oxidative DNA damage in the parkinsonian brain: an apparent selective increase in 8-hydroxyguanine levels in substantia nigra. J Neurochem 69(3):1196–1203
6. Schapira AHV (2007) Mitochondrial dysfunction in Parkinson's disease. Cell Death Differ 14(7):1261–1266
7. Smeyne M, Smeyne RJ (2013) Glutathione metabolism and Parkinson's disease. Free Radic Biol Med 62:13–25, **Review**
8. Piccini P, Burn DJ, Ceravolo R, Maraganore D, Brooks DJ (1999) The role of inheritance in sporadic Parkinson's disease: evidence from a longitudinal study of dopaminergic function in twins. Ann Neurol 45(5):577–582
9. Elbaz A, Dufouil C, Alpérovitch A (2007) Interaction between genes and environment in neurodegenerative diseases. C R Biol 330(4):318–328, **Review**
10. Kieburtz K, Wunderle KB (2013) Parkinson's disease: evidence for environmental risk factors. Mov Disord 28(1):8–13, **Review**
11. Gorell JM, Johnson CC, Rybicki BA, Peterson EL, Richardson RJ (1998) The risk of Parkinson's disease with exposure to pesticides, farming, well water, and rural living. Neurology 50(5):1346–1350
12. Savitz DA, Checkoway H, Loomis DP (1998) Magnetic field exposure and neurodegenerative disease mortality among electric utility workers. Epidemiology 4:398–404
13. Davanipour Z, Tseng CC, Lee PJ, Sobel E (2007) A case-control study of occupational magnetic field exposure and Alzheimer's disease: results from the California Alzheimer's Disease Diagnosis and Treatment Centers. BMC Neurol 7:13
14. Li CY, Sung FC (2003) Association between occupational exposure to power frequency electromagnetic fields and amyotrophic lateral sclerosis: a review. Am J Ind Med 43(2):212–220
15. Consales C, Merla C, Marino C, Benassi B (2012) Electromagnetic fields, oxidative stress, and neurodegeneration. Int J Cell Biol 2012: 683897
16. Wechsler LS, Checkoway H, Franklin GM, Costa LG (1991) A pilot study of occupational and environmental risk factors for Parkinson's disease. Neurotoxicology 12(3):387–392
17. Adair RK (1999) Effects of very weak magnetic fields on radical pair reformation. Bioelectromagnetics 20(4):255–263
18. Samano JM, Torres-Duran PV, Juarez-Oropeza MA, Verdugo-Diaz L (2012) Effects of acute extremely low frequency electromagnetic field exposure on the antioxidant status and lipid levels in rat brain. Arch Med Res 43:183–189
19. Di Loreto S, Falone S, Caracciolo V, Sebastiani P, D'Alessandro A, Mirabilio A, Zimmitti V, Amicarelli F (2009) Fifty hertz extremely low-frequency magnetic field exposure elicits redox and trophic response in rat-cortical neurons. J Cell Physiol 219(2):334–343
20. Morabito C, Guarnieri S, Fanò G, Mariggiò MA (2010) Effects of acute and chronic low frequency electromagnetic field exposure on PC12 cells during neuronal differentiation. Cell Physiol Biochem 26(6):947–958
21. Falone S, Grossi MR, Cinque B, D'Angelo B, Tettamanti E et al (2007) Fifty Hertz extremely low frequency electromagnetic field causes changes in redox and differentiative status in neuroblastoma cells. Int J Biochem Cell Biol 39(11):2093–2106
22. Beal MF (2001) Experimental models of Parkinson's disease. Nat Rev Neurosci 2(5):325–334, **Review**
23. Langston JW, Ballard PA Jr (1983) Parkinson's disease in a chemist working with 1-methyl-4-phenyl-1,2,5,6-tetrahydropyridine. N Engl J Med 309(5):310
24. Burns RS, Chiueh CC, Markey SP, Ebert MH, Jacobowitz DM, Kopin IJ (1983) A primate model of parkinsonism: selective destruction of dopaminergic neurons in the pars compacta of the substantia nigra by N-methyl-4-phenyl-1,2,3,6-tetrahydropyridine. Proc Natl Acad Sci U S A 80(14):4546–4550
25. Suzuki K, Mizuno Y, Yoshida M (1990) Effects of 1-methyl-4-phenyl-1,2,3,6-tetrahydropyridine (MPTP)-like compounds on mitochondrial respiration. Adv Neurol 53:215–218
26. Presgraves SP, Ahmed T, Borwege S, Joyce JN (2004) Terminally differentiated SH-SY5Y cells provide a model system for studying neuroprotective effects of dopamine agonists. Neurotox Res 5(8): 579–598
27. Lodato R, Merla C, Pinto R, Mancini S, Lopresto V, Lovisolo GA (2013) Complex magnetic field exposure system for in vitro experiments at intermediate frequencies. Bioelectromagnetics 34(3):211–219
28. Schuderer J, Oesch W, Felber N, Spät D, Kuster N (2004) In vitro exposure apparatus for ELF magnetic fields. Bioelectromagnetics 25(8):582–591
29. Kuster N, Schuderer J, Christ A, Futter P, Ebert S (2004) Guidance for exposure design of human studies addressing health risk evaluations of mobile phones. Bioelectromagnetics 25(7):524–529
30. Cardaci S, Filomeni G, Rotilio G, Ciriolo MR (2010) $p38^{MAPK}$/p53 signaling axis mediates neuronal apoptosis in response to tetrahydrobiopterin-induced oxidative stress and glucose uptake inhibition: implication for neurodegeneration. Biochem J 430:439–451
31. Filomeni G, Graziani I, De Zio D, Dini L, Centonze D, Rotilio G, Ciriolo MR (2012) Neuroprotection of kaempferol by autophagy in models of rotenone-mediated acute toxicity: possible implications for Parkinson's disease. Neurobiol Aging 33(4):767–785
32. Poot M, Kavanagh TJ, Kang HC, Haugland RP, Rabinovitch PS (1991) Flow cytometric analysis of cell cycle-dependent changes in cell thiol level by combining a new laser dye with Hoechst 33342. Cytometry 12(2):184–187
33. Darzynkiewicz Z, Juan G, Li X, Gorczyca W, Murakami T, Traganos F (1997) Cytometry in cell necrobiology: analysis of apoptosis and accidental cell death (necrosis). Cytometry 27(1):1–20
34. Wilkins RC, Kutzner BC, Truong M, Sanchez-Dardon J, McLean JR (2002) Analysis of radiation-induced apoptosis in human lymphocytes: flow cytometry using Annexin V and propidium iodide versus the neutral comet assay. Cytometry 48(1):14–19
35. Metkar S, Wang B, Catalan E, Anderluh G, Gilbert RJ, Pardo J, Froelich CJ (2011) Perforin rapidly induces plasma membrane phospholipid flip-flop. PLoS One 6(9), e24286
36. Wong CM, Cheema AK, Zhang L, Suzuki YJ (2008) Protein carbonylation as novel mechanism in redox signaling. Circ Res 102: 310–318
37. Nicotra A, Parvez S (2002) Apoptotic molecules and MPTP-induced cell death. Neurotoxicol Teratol 24(5):599–605
38. Xie HR, Hu LS, Li GY (2010) SH-SY5Y human neuroblastoma cell line: in vitro cell model of dopaminergic neurons in Parkinson's disease. Chin Med J (Engl) 123(8):1086–1092, **Review**
39. Korecka JA, van Kesteren RE, Blaas E, Spitzer SO, Kamstra JH, Smit AB, Swaab DF, Verhaagen J et al (2003) Phenotypic characterization of retinoic acid differentiated SH-SY5Y cells by transcriptional profiling. PLoS One 8(5), e63862
40. Wertheimer N, Leeper E (1979) Electrical wiring configurations and childhood cancer. Am J Epidemiol 109(3):273–284
41. Loomis DP, Savitz DA (1990) Mortality from brain cancer and leukaemia among electrical workers. Br J Ind Med 47(9):633–638
42. Mattsson MO, Simkò (2012) Is there a relationship between extremely low frequency magnetic field exposure, inflammation and neurodegenerative diseases? A review of in vivo and in vitro experimental evidences. Toxicology 301:1–12
43. Di Lazzaro V, Capone F, Apollonio F, Borea PA, Cadossi R, Fassina L, Grassi C, Liberti M et al (2013) A consensus panel review of central nervous system effects of the exposure to low-intensity extremely low frequency magnetic fields. Brain Stimul 6:469–476
44. Gordon J, Amini S, White MK (2013) General overview of neuronal cell culture. Methods Mol Biol 1078:1–8

45. International Commission on Non-Ionizing Radiation Protection (2010) Guidelines for limiting exposure to time-varying electric and magnetic fields (1 Hz to 100 kHz). Health Phys 99(6):818–836
46. Reale M, Kamal MA, Patruno A, Costantini E, D'Angelo C, Pesce M, Greig NH (2014) Neuronal cellular responses to extremely low frequency electromagnetic field exposure: implications regarding oxidative stress and neurodegeneration. PLoS One 9(8), e104973
47. Luukkonen J, Liimatainen A, Juutilainen J, Naarala J (2014) Induction of genomic instability, oxidative processes, and mitochondrial activity by 50Hz magnetic fields in human SH-SY5Y neuroblastoma cells. Mutat Res Fundam Mol Mech Mutagen 760:33–41
48. Cadet JL, Brannock C (1998) Free radicals and the pathobiology of brain dopamine systems. Neurochem Int 32:117–131
49. Infanger DW, Sharma RV, Davisson RL (2006) NADPH oxidases of the brain: distribution, regulation, and function. Antioxid Redox Signal 8(9-10):1583–1596, **Review**
50. Pearce RK, Owen A, Daniel S, Jenner P, Marsden CD (1997) Alterations in the distribution of glutathione in the substantia nigra in Parkinson's disease. J Neural Transm 104(6-7):661–677
51. Jellinger KA (2008) A critical reappraisal of current staging of Lewy-related pathology in human brain. Acta Neuropathol 116:1–16
52. Chinta SJ, Andersen JK (2006) Reversible inhibition of mitochondrial complex I activity following chronic dopaminergic glutathione depletion in vitro: implications for Parkinson's disease. Free Radic Biol Med 41:1442–1448
53. Holmay MJ, Terpstra M, Coles L, Mishra U, Ahlskog M, Oz G, Cloyd JC, Tuite PJ (2013) N-acetylcysteine boosts brain and blood glutathione in Gaucher and Parkinson disease. Clin Neuropharmacol 36(4):103–106
54. Berman AE, Chan WY, Brennan AM et al (2011) N-acetylcysteine prevents loss of dopaminergic neurons in the EAAC1$^{-/-}$ mouse. Ann Neurol 69:509–520
55. Wüllner U, Löschmann PA, Schulz JB, Schmid A, Dringen R, Eblen F, Turski L, Klockgether T (1996) Glutathione depletion potentiates MPTP and MPP+ toxicity in nigral dopaminergic neurones. Neuroreport 7(4):921–923
56. Bizzozero OA, Ziegler JL, De Jesus G, Bolognani F (2006) Acute depletion of reduced glutathione causes extensive carbonylation of rat brain proteins. J Neurosci Res 83(4):656–667
57. Chinta SJ, Kumar MJ, Hsu M et al (2007) Inducible alterations of glutathione levels in adult dopaminergic midbrain neurons result in nigrostriatal degeneration. J Neurosci 27:13997–14006
58. Ma Q, Deng P, Zhu G, Liu C, Zhang L, Zhou Z, Luo X, Li M et al (2014) Extremely low frequency electromagnetic fields affect transcript levels of neuronal differentiation-related genes in embryonic neural stem cells. PLoS One 9(3), e90041
59. Manikonda PK, Rajendrap, Devendranath D, Gunasekaran B, Channakeshava, Aradhya RS, Sashidar RB, Subramanyam C (2007) Influence of the extremely low frequency magnetic field and $Ca^{2+}$ signaling and NMDA receptor in rat hippocampus. Neurosci Lett 413(2):145–149